Lasers in Medical Science (2020) 35:413–420
https://doi.org/10.1007/s10103-019-02838-w

ORIGINAL ARTICLE

Comparative effects of photobiomodulation therapy at wavelengths of 660 and 808 nm on regeneration of inferior alveolar nerve in rats following crush injury

Nurettin Diker[1] · Duygu Aytac[2] · Fatma Helvacioglu[3] · Yener Oguz[4]

Received: 26 February 2019 / Accepted: 25 June 2019 / Published online: 4 July 2019

Abstract

The aim of the present study was to investigate the therapeutic effects of 660-nm and 880-nm photobiomodulation therapy (PBMT) following inferior alveolar nerve (IAN) crush injury. Following the nerve crush injuries of IAN, 36 Wistar rats were randomly divided into three groups as follows: (1) control, (2) 660-nm PBMT, and (3) 808-nm PBMT (GaAlAs laser, 100 J/cm^2, 70 mW, 0.028-cm^2 beam). PBMT was started immediately after surgery and performed once every 3 days during the postoperative period. At the end of the 30-day treatment period, histopathological and histomorphometric evaluations of tissue sections were made under a light and electron microscope. The ratio of the inner axonal diameter to the total outer axonal diameter (*g*-ratio) and the number of axons per square micrometer were evaluated. In the 808-nm PBMT group, the number of nerve fibers with suboptimal *g*-ratio ranges of 0–0.49 ($p < 0.001$) is significantly lower than expected, which indicates better rate of myelinization in the 808-nm PBMT group. The number of axons per square micrometer was significantly higher in the 808-nm PBMT group when compared with the control ($p < 0.001$) and 660-nm PBMT group ($p = 0.010$). The data and the histopathological investigations suggest that the PBMT with the 808-nm wavelength along with its settings was able to enhance IAN regeneration after nerve crush injury.

Keywords Photobiomodulation · Wavelength · Inferior alveolar nerve · Nerve injury · Biostimulation

Introduction

Inferior alveolar nerve (IAN) is the largest branch of the mandibular nerve. It is positioned in the mandibular canal that extends from the mandibular foramen to the mental foramen. Third molar surgeries [1], dental implant surgeries [2], endodontic treatments [3], injection of local analgesics [4], surgeries for correcting dentofacial anomalies [5], dentofacial trauma [6], and pathologies of jaws [7] can be listed as IAN injury etiologies. Nerve injuries may produce a wide spectrum of neurological alterations from total anesthesia to painful situations, like dysesthesia and allodynia [8]. Permanent sequelae after nerve injuries of the maxillofacial region may significantly affect the patients' quality of life via influencing the patients' speech, chewing, and social interactions [9] and may cause legal disputes between patients and surgeons.

Complete nerve lacerations and avulsions require early reconstruction of IAN via microsurgical approaches. End-to-end connection and nerve grafting are the two major techniques used [10]. To control the inflammatory reactions in the damaged nerve, a course of steroid or non-steroidal anti-inflammatory drugs can be prescribed [11]. However, with the treatments available today, complete recovery is uncommon and not always satisfactory [10]. The development of alternative adjuvant therapies is necessary to improve the recovery process of IAN.

✉ Nurettin Diker
ndiker@bezmialem.edu.tr; dikernurettin7tp@gmail.com

[1] Department of Oral and Maxillofacial Surgery, Faculty of Dentistry, Bezmialem Vakif University, Adnan Menderes Bulvarı, Vatan Caddesi, 34093 Fatih, Istanbul, Turkey

[2] Private Practice, Cankaya Mahallesi, Cankaya Caddesi No. 10/3 Cankaya, Ankara, Turkey

[3] Department of Histology and Embryology, Baskent University, Fatih Sultan Mahallesi, Eskişehir Yolu 18 km 06790 Etimesgut, Ankara, Turkey

[4] Private Practice, Drs. Nicolas & ASP Dental Center, Jumeirah Beach Road, Dubai, United Arab Emirates

Effects of photobiomodulation therapy (PBMT) are related to tissue biostimulation, presenting therapeutic responses from photoelectric, photoenergetic, and photochemical reactions [12]. One of the main mechanisms of PBMT rests on photon absorption by cytochrome c oxidase (CCO) which is the terminal enzyme of electron transport chain and plays a vital role in the neuronal oxygen utilization for energy metabolism [13]. The absorption of photons by CCO increases the oxygen consumption and production of ATP via mitochondrial oxidative phosphorylation [14].

In clinical medicine, PBMT which is formerly referred as low-level laser therapy (LLLT), was introduced to promote the repair and recovery of tissues. PBMT is also related to the prevention of tissue death, pain relief, and reduction of inflammation [15, 16]. PBMT is currently being investigated in an attempt to achieve early functional recovery after peripheral nerve injuries. A Cochrane review examined the interventions for iatrogenic IAN injuries and concluded that LLLT is the only evidence-based treatment modality with very low quality of evidence [17]. However, PBMT remains controversial for many clinicians because it presents difficulties in selecting the most effective parameters for the intended treatment due to lack of standardization. The wavelength is one of the key points for PBMT that regulates the depth and penetration of the laser irradiance into the tissue [15]. Therefore, our study is aimed at evaluating the effects of varying wavelengths on IAN regeneration following crush injury.

Material and methods

Animals and surgical procedure

This study was approved by the Institutional Review Board and Ethical Committee of Baskent University for experimental research on animals (Project no. D-DA 14/06) and supported by the Baskent University Research Fund. Thirty-six 12-week-old female Wistar rats were obtained from the animal experiment center of Baskent University. Animals were kept on a 12-h day/night cycle and maintained ad libitum on water and standard laboratory aliment. Animals were anesthetized by intraperitoneal injection of ketamine (60 mg/kg) and xylazine (6 mg/kg) combination. Preoperative enrofloxacin (10 mg/kg, intramuscular) and fentanyl (0.02 mg/kg, subcutaneous) were also given. Throughout the procedure, a thermal blanket kept to 37 °C and rectal temperature measurement were employed to control body temperature. Rats were immobilized on the operation table in a sideward position. Ten-millimeter vertical incisions that start 5 mm below the lateral canthus of the eye were performed. For achieving access to the lateral side of the mandibular ramus, the masseter was bluntly dissected immediately below the parotid's salivary duct with the sharp pointed microforceps (Bahadir D 105.00, Samsun, Turkey). The bone over the mandibular canal was removed with a rotary instrument (Saeshin, Strong 204, Mainland, China) and tungsten carbide burs (US1-HP 008, Meisinger, Neuss, Germany) under serum physiologic irrigation. The IAN injury was induced at the level of 2 mm rostral to the mandibular foramen where the main trunk of IAN divided into two large branches [18]. The IAN was clamped for thirty seconds with microforceps (Bahadir D 103.00, Samsun, Turkey) to induce crush injury. Right IANs of rats were subjected to injury model and left IANs were kept intact.

Irradiation procedures

Animals were randomly divided into three groups, twelve rats per group. A gallium-aluminum-arsenide (GaAlAs) diode laser (DMC Whitening Lase II, Sao Carlos, Brazil) was used at 660-nm or 808-nm wavelength for the irradiation groups. The other laser parameters were the same for both the treatment groups as shown in Table 1. The probe was placed on the buccal skin surface, directly above the site of injury, without skin contact. The treatment protocol for the control group was the same as the laser-irradiated group, but the device was not switched on. PBMT was started immediately after surgery and performed once every 3 days during the postoperative period. The tenth session was applied at the 27th postoperative day. Nerve samples from the distal part of the injury were harvested at the 30th postoperative day, and then, the animals were sacrificed.

Histopathological and histomorphometric analysis

Harvested nerve tissues were fixed in a phosphate-buffered solution (pH 7.3) containing 2.5% glutaraldehyde (Sigma-Aldrich Co., St. Louis, USA) for 2 h at room temperature, post-fixed in 1% osmium tetroxide (Sigma-Aldrich Co.), and dehydrated in a series of graded alcohols (50, 60, 70, 80, 90, and 100% ethanol). After passing through propylene oxide (Sigma-Aldrich Co.), specimens were embedded in Araldite CY 212 (Ciba-Geigy, Delhi, India), (2-dodecen-1-yl) succinic anhydride (Sigma-Aldrich Co.), benzyldimethyl amine (Polysciences Inc., Philadelphia, USA), and dibutylphthalate (Sigma-Aldrich Co.). The semi-thin sections were stained with toluidine blue (Sigma-Aldrich Co.) and examined with a photomicroscope (DM 500 Leica, Wetzlar, Germany). After the selection of appropriate specimens, thin sections were cut and stained with uranyl acetate (ProSciTech, Townsville, Australia) and lead citrate (Sigma-Aldrich Co.). Samples were histopathologically examined under an electron microscope (Leo 906 E Carl Zeiss, Göttingen, Germany) at × 6000 magnification by two histologists who were blinded to the sample group.

Table 1 Laser device parameters

Parameter	Value
Device information	
Manufacturer	DMC
Model identifier	Whitening Lase II
Emitter type	GaAlAs
Irradiation parameters	
Beam shape	Circular
Wavelength	660 nm vs. 808 nm
Operating mode	Pulsed wave
Frequency	50 Hz
Peak radiant power	100 mW
Average radiant power	70 mW
Beam shape	Circular
Treatment parameters	
Beam spot size	0.028 cm^2
Irradiance at target	2.5 W/cm^2
Exposure duration	80 s
Radiant exposure	100 J/cm^2
Radiant energy	2.7 J/session
Number of points irradiated	One
Application technique	Non-contact mode
Number and frequency of treatment sessions	10 treatments in total, delivered once 3 days over 30 days
Total radiant energy	27 J

Histomorphometric evaluation of the *g*-ratio for the myelinated axons was made in the semi-thin sections at × 1000 magnification. Figures of randomly selected fields of transverse sections were drawn. The *g*-ratio was calculated by dividing the inner axonal diameter by the outer fiber diameter, and the results were stratified in ranges of 0–0.49, 0.50–0.54, 0.55–0.69, and 0.7–1. *g*-ratio values between 0.55 and 0.69 were considered to be in the optimal range [19]. Quantifications were performed using the Tantuna 76 software (Baskent University Department of Biophysics, Ankara, Turkey). Axonal density was evaluated in the semi-thin sections at × 100 magnification using ImageJ software (ImageJ 1.48v; National Institutes of Health, Bethesda, MD). The total number of axons in each section was counted and divided by the total area.

Statistical analysis

The *g*-ratio results are expressed as numbers (*n*) and percentages (*p*). Categorical data were analyzed with Fisher's exact test and the Chi-squared test. Where expected frequencies were less than 5, the Monte Carlo simulation method was performed. Axonal densities are expressed as mean ± SD and analyzed with one-way ANOVA and Tukey's post hoc test. p values < 0.05 were considered to indicate statistical significance. Sample size, axonal density results, and the significance level of the present study provided 98% power according to results of the post hoc power analysis. Statistical analyses were carried out using PASW 18.0 software (SPSS, USA).

Results

Recovery from anesthesia and surgical intervention was uneventful. No postoperative complications were observed. All animals tolerated laser irradiation well and survived until the final experimental time.

Histomorphometric analysis

g-ratio values in the 808-nm PBMT groups presented better results, since most axon fibers fell into optimal *g*-ratio range (0.55–0.69). The control group showed a significantly higher number of axons concentrated in the *g*-ratio range of 0–0.49, which indicates insufficient myelinization ($p = 0.001$).

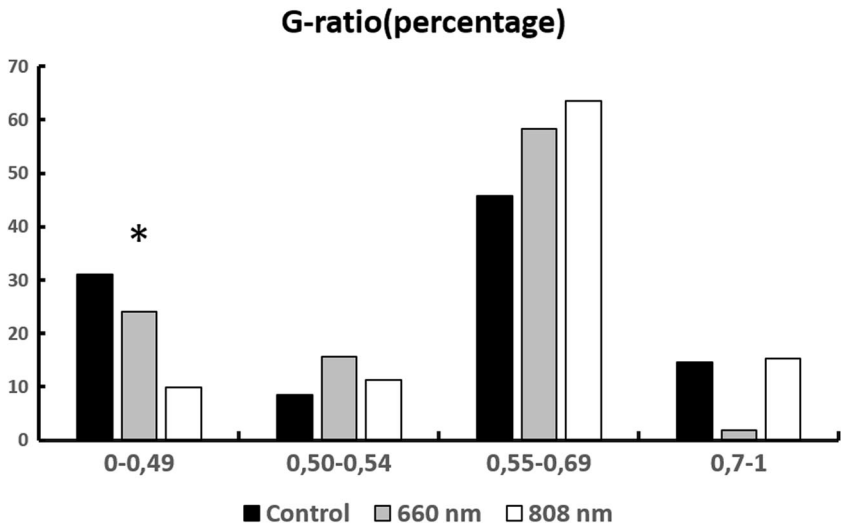

Fig. 1 Results of *g*-ratio distribution. The control group showed significantly higher concentration of axons in the *g*-ratio range of 0–0.49 ($p = 0.001$). In the 808-nm PBMT group, the number of nerve fibers with sub-optimal *g*-ratio ranges of 0–0.49 ($p < 0.001$) is significantly lower than expected

However, in the 808-nm PBMT group, the number of nerve fibers with suboptimal *g*-ratio ranges of 0–0.49 ($p < 0.001$) is significantly lower than expected, which indicates a better rate of myelinization in the 808-nm PBMT group (Fig. 1).

The number of axons per unit square micrometer was significantly higher in the 808-nm group when compared with the control group ($p < 0.001$). In addition, a significantly higher axonal density was observed in the 808-nm PBMT group compared with the 660-nm PBMT group ($p = 0.010$). However, histomorphometric analysis of axon density revealed no significant differences between the 660-nm PBMT group and the control group ($p = 0.295$) (Fig. 2).

Histopathological analysis

Histopathological analysis of the control group revealed a higher number of degenerative injuries in the myelinated nerve fibers compared with the treatment groups. Electron microscopy analysis revealed that larger-diameter nerve fibers in the control group were not able to preserve their physiological nerve fiber structure. Severe degenerative changes were noted in the myelin sheaths of large-diameter axons. More than one myelinated nerve fiber was observed in the cytoplasm of a few Schwann cells, which is uncommon. Two myelin sheaths with different thicknesses in their polyaxonal Schwann cells were noted during investigation of the thin sections. Collagen fiber deposition in the intercellular space was evident in the whole tissue sections compared with the treatment groups (Fig. 3a).

During the investigation of the tissue sections in the 660-nm PBMT group, myelin remnants in the cytoplasm of the myelinated axons were observed, similar to the control group. Cellular remnants engulfed by phagocytes were observed in close proximity to severely degenerated myelin sheaths. Edema was significant in the intercellular space. Collagen

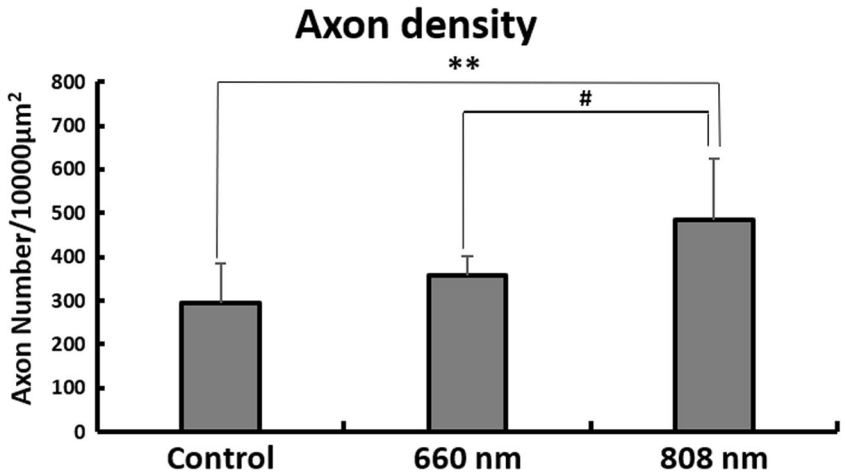

Fig. 2 Results of axonal density in semi-thin sections of the nerves. The number of axons per unit square micrometer was significantly higher in the 808-nm group when compared with the control group ($p < 0.001$) and 660-nm PBMT group ($p = 0.010$). Analysis of the axon density results revealed no significant differences between the 660-nm PBMT group and the control group ($p = 0.295$). Data are mean values ± S.D. $^{**}p < 0.01$ versus control samples; # $p < 0.05$ versus the 660-nm PBMT group

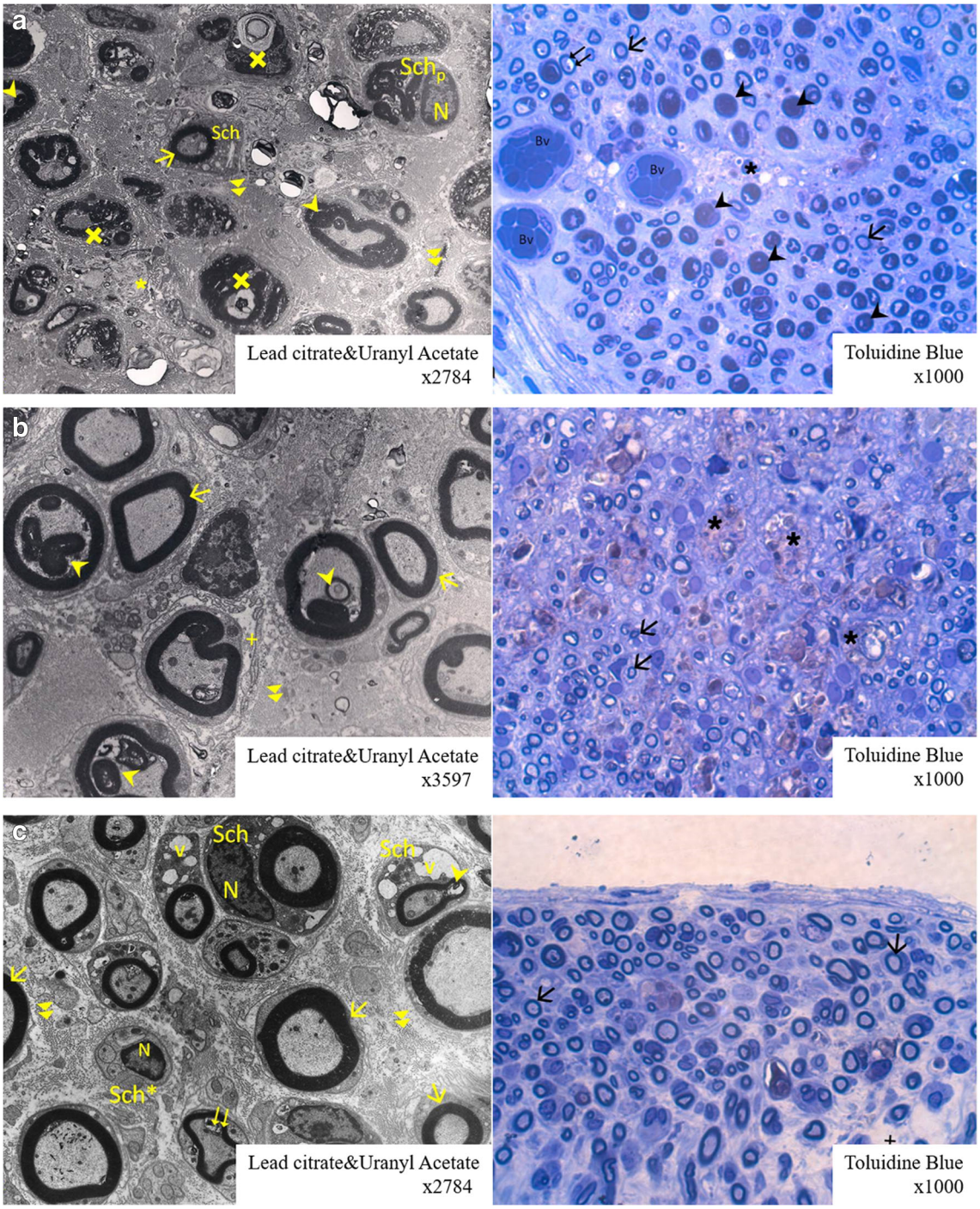

Fig. 3 Representative images of thin and semi-thin sections of the nerves. **a** The control group demonstrating multiple polyaxonal Schwann cells, severe degenerative changes in the myelin sheaths of large diameter axons, and prominent collagen fiber deposition in the intercellular space. **b** The 660-nm PBMT group demonstrating engulfed cellular remnants by phagocytes, edema, and collagen fiber deposition in the intercellular space. **c** The 808-nm PBMT group demonstrating accumulation of small membrane-bounded vacuoles, higher number of the myelinated axons with physiological structure, relatively lower edema, and collagen fiber deposition. → structurally normal myelinated nerve fiber, ⇉ axonal retraction of myelinated nerve fiber, Bv capillary blood vessel, ✱ cellular remnants phagocyted by macrophages, **X** degenerative myelinated nerve fiber, ➤ myelin sheaths with different thicknesses within a myelinated nerve axon, ⏩ collagen fiber in the intercellular connective tissue, + edema in the intercellular connective tissue, Sch Schwann cell, Sch* degenerative Schwan cell, Sch_P polyaxonal Schwann cell, N nucleus of Schwann cell, v vacuole, m non-myelinated nerve fiber.

fiber deposition in the intercellular space was evident where edema was not noted (Fig. 3b).

Tissue sections of the 808-nm PBMT group revealed that the general structure of the nerve was preserved, and a relatively higher number of the myelinated axons with physiological structure were noted when compared with the other groups. In addition, edema and collagen fiber deposition were relatively lower in the intercellular connective tissue (Fig. 3c).

Discussion

Photobiomodulation therapy exerts biostimulatory effects and is indicated in a variety of clinical conditions, such as osteoarthritis, lower back pain, temporomandibular joint disorders, and ulcers [20]. It is a non-invasive procedure and can be used alone or in combination with other indicated therapies. The advantages of PBMT include limited contraindications for application, no adverse effect, and easy application [21]. PBMT has been used in several clinical and experimental studies on peripheral nerve regeneration. It has been shown that PBMT can enhance the postinjury functionality, increase the axonal diameter, increase the thickness of myelin sheath, diminish the inflammatory reaction, and increase the neurotrophic growth factors following peripheral nerve injury [22]. Gasperini et al. [23] showed that combined 660-nm and 789-nm wavelength LLLT can accelerate the recovery of IAN after bilateral sagittal split osteotomies (BSSO) of the mandible in the early postoperative period compared with the non-irradiated IANs on the other side of the mandible. Guarini et al. [24] observed that photobiomodulation with 810-nm GaAlAs laser irradiation enhanced the neurosensory recovery of IAN at the end of 2 years after BSSO.

Lasers using different wavelengths are being developed and researched, which can emit in the range of 400–1100 nm [25]. The most commonly used wavelengths for PBMT can be classified into visible light (400–700 nm) and near-infrared (NIR) light (700–1100 nm) [20].

In the present experimental study, the regenerative effects of GaAlAs laser irradiation with 660 nm (in the red light spectral region) and 808 nm (in the NIR spectral region) were compared following crush injury of IAN. The histopathological investigation revealed that laser treatment with 660-nm wavelength irradiation was insufficient to reverse the morphological degenerative changes after nerve injury, while the 808-nm wavelength irradiation relatively suppressed the edema and collagen fiber deposition in the intercellular spaces and preserved the physiologic structure of the myelinated and unmyelinated nerve fibers. In the 808-nm group, the percentage of nerve fibers with suboptimal *g*-ratio ranges of 0–0.49 and 0.7–1 was significantly low than expected, which indicates better rate of myelinization. In agreement with the histopathological investigations, the results of the histomorphometric investigations indicated that 808-nm wavelength irradiation enhanced the axonal density and myelin maturation during regeneration of the injured nerve.

Wavelengths in the NIR spectral region are the most frequently used and investigated wavelengths for peripheral nerve regeneration. Effects of 780-nm wavelength on the regeneration of the injured sciatic nerve were investigated in a previous research, where accelerated revascularization and decreased Wallerian degeneration with higher axonal density were noted [26]. Wang et al. used laser at 808 nm and 8 J/cm^2 for the recovery of sciatic nerves in rats following crush injury; treatment was provided for 20 days consecutively, and western blot analysis showed a significantly higher GAP43 protein expression, which is normally expressed at high levels in the neuronal growth cones during axonal regeneration [27].

In addition to researches on PBMT at wavelengths in the NIR spectral region, regenerative effects of the wavelengths in the visible light spectral region were also investigated in a few researches. Takhtfooladi et al. reported a significant improvement in the functional recovery of the sciatic nerve after 21 days of treatment with 685-nm LLLT at a dosage of 3 J/cm^2 [28]. The effects of 680-nm LLLT, 650-nm red LED, and 450-nm blue LED treatments on the regeneration of the transected sciatic nerve after an end-to-end neurorrhaphy were evaluated in another study by Takhtfooladi et al. Results of the 685-nm LLLT group showed an increased number of neurons and myelinated axons compared with the other groups [29].

Comparison of 660-nm and 808-nm wavelength irradiation was performed following complete nerve resection in an experimental study, and interestingly, enhanced functional recovery and enhanced fiber diameter were noted in the 660-nm wavelength irradiation group, while histomorphometric results of the 808-nm wavelength irradiation group indicated higher fiber density in the tissue sections [30]. Barbosa et al. compared the regenerative effects of 660-nm and 830-nm laser irradiation following sciatic nerve crush injury and noted enhanced functional recovery on the 14th postoperative day in 660-nm laser irradiation group, while no differences were observed between sham, 660-nm, and 830-nm groups on the 21st postoperative day [31].

There have been contradictory results in previous studies about the optimum wavelength of PBMT for nerve regeneration. However, most of these studies were performed on sciatic nerves of animals, and only a few experimental studies were conducted to investigate the effects of PBMT following IAN injury. Martins et al. evaluated the effects of a gallium arsenide laser, emitting a wavelength of 904 nm, following IAN injury by conducting two consecutive researches [32, 33]. It was reported that the 904-nm laser irradiation improved the nociceptive behavior of rats; decreased the brain-derived neurotrophic factor, which plays a crucial role in pain-related behavior development; and increased the nerve growth factor, which is involved in the regeneration of sensory nerves [32].

In addition to the enhanced nociceptive behavior, laser irradiations with the same parameters enhanced the myelin sheath thickness, nerve fiber diameter, and axon diameter [33]. To the best of our knowledge, the present study is the first experimental study that investigated the effects of different wavelengths on the regeneration of IAN and concluded that laser irradiation with 808-nm wavelength is superior to laser irradiation with 660 nm.

Wavelengths in the 600–700-nm range are preferred for treating superficial tissues, and wavelengths between 780 and 950 nm are chosen for deeper-seated tissues due to longer optical penetration distance through the tissue [29]. The fundamental reason for the different penetration depths is the absorption of the laser via melanin. Maximal melanin absorption occurs at wavelengths shorter than 510 nm, but the absorption is still prominent for red light (600–700 nm). However, the effect of melanin becomes negligible in the NIR spectral region, beyond 800 nm. Souza-Barros et al. reported greater transmittance at 808-nm than 635-nm wavelength, regardless of skin thickness [34]. In order to have a successful therapy, laser power should be effectively delivered to the target layer of the tissue without any considerable absorption in other layers [35]. In addition to the absorption of laser irradiation in the different layers of skin, further penetration of laser irradiation may be necessary to achieve successful regeneration of IAN injury due to its anatomic position. Laser irradiation has to pass through the outer layer of the mandibular bone to reach IAN that is located in the mandibular canal.

The number of interventional PBMT treatments and the interval between sessions have varied in the literature. Miloro and Criddle stated that 20 sessions over a 3-month period are accepted as standard practice for treatment of IAN injury in humans [36]. In another study of Miloro et al., LLLT protocol was repeated at 6 h, once per day for 4 days, and once a week for 1 month, for a total of 10 treatments to enhance regeneration of segmental IAN defects of rabbits, and results were evaluated at the end of 15 weeks [37]. In the present study, crush injury was induced and a total of 10 PBMT sessions were applied with regular intervals over a 30-day period. In this 30-day period, most of the regeneration is expected to occur, and the regenerative effects of the treatment can be observed after crush injury of IAN in rats. The excepted regeneration time differs between the type of injury, investigated nerve, and investigated species [38], which make it difficult to compare treatment protocols across the literature. Further studies are needed to establish exact PBMT protocols for different clinical scenarios of nerve injury.

There may be some possible limitations in this study. Induced heat during application of PBMT was not evaluated in the present study. However, rigorously modeling temperature change is quite challenging during in vivo studies and the study of Wang et al. concluded that CCO activity was not significantly modified by heat stimulation caused by the interaction of laser and tissue [39]. Wavelength is not the only parameter that affects the efficacy of PBMT. Other parameters, such as power, dose, and type of laser, are also strongly correlated with the efficacy of PBMT. Unfortunately, many of previous studies did not describe the necessary parameters of laser irradiation, such as the dose, power, duration of irradiation, and manner of application. This leads to difficulties in comparing different studies and may be responsible for the contradictory results.

Conclusion

Based on the histomorphometric and histopathological results of the present study, it can be concluded that the 808-nm wavelength PBMT along with the parameters used in this study presented positive effects on IAN regeneration at the end of 30-day healing period. Thus, the 808-nm wavelength PBMT, with higher penetration capacity through the tissues, is advantageous for biostimulation of IAN following injury. Further studies should be carried out to define the optimum PBMT parameters for the biostimulation of IAN.

Funding This research was funded by Baskent University Research Fund (Grand Number D-DA 14/06).

Compliance with ethical standards

Conflict of interest The authors declare that they have no conflict of interest.

Ethical approval All procedures performed in the present study, involving animals, were approved by the Institutional Review Board and Ethical Committee of Baskent University for experimental research on animals.

References

1. Bataineh AB (2001) Sensory nerve impairment following mandibular third molar surgery. J Oral Maxillofac Surg 59:1012–1017
2. Ellies LG, Hawker PB (1993) The prevalence of altered sensation associated with implant surgery. Int J Oral Maxillofac Implants 8: 674–679
3. Grötz KA, Al-Nawas B, de Aguiar EG et al (1998) Treatment of injuries to the inferior alveolar nerve after endodontic procedures. Clin Oral Investig 2:73–76
4. Haas DA (2006) Articaine and paresthesia: epidemiological studies. J Am Coll Dent 73:5–10
5. McLeod NMH, Bowe DC (2016) Nerve injury associated with orthognathic surgery. Part 2: inferior alveolar nerve. Br J Oral Maxillofac Surg 54:366–371
6. Tay ABG, Bin LJ, Lye KW et al (2015) Inferior alveolar nerve injury in trauma-induced mandible fractures. J Oral Maxillofac Surg 73:1328–1340
7. Sumer M, Bas B, Yıldız L (2007) Inferior alveolar nerve paresthesia caused by a dentigerous cyst associated with three teeth. Med Oral Patol Oral Cir Bucal 12:E388–E390

8. Schultze-Mosgau S, Reich RH (1993) Assessment of inferior alveolar and lingual nerve disturbances after dentoalveolar surgery, and of recovery of sensitivity. Int J Oral Maxillofac Surg 22:214–217
9. Long H, Zhou Y, Liao L et al (2012) Coronectomy vs. total removal for third molar extraction: a systematic review. J Dent Res 91:659–665
10. Leung YY, Fung PP-L, Cheung LK (2012) Treatment modalities of neurosensory deficit after lower third molar surgery: a systematic review. J Oral Maxillofac Surg 70:768–778
11. Alhassani AA, AlGhamdi AST (2010) Inferior alveolar nerve injury in implant dentistry: diagnosis, causes, prevention, and management. J Oral Implantol 36:401–407
12. Angeletti P, Pereira MD, Gomes HC et al (2010) Effect of low-level laser therapy (GaAlAs) on bone regeneration in midpalatal anterior suture after surgically assisted rapid maxillary expansion. Oral Surg Oral Med Oral Pathol Oral Radiol Endod 109:e38–e46
13. Wang X, Tian F, Reddy DD et al (2017) Up-regulation of cerebral cytochrome-c-oxidase and hemodynamics by transcranial infrared laser stimulation: a broadband near-infrared spectroscopy study. J Cereb Blood Flow Metab 37:3789–3802
14. Rojas JC, Gonzalez-Lima F (2013) Neurological and psychological applications of transcranial lasers and LEDs. Biochem Pharmacol 86:447–457
15. de Rosso MPO, Buchaim DV, Kawano N et al (2018) Photobiomodulation therapy (PBMT) in peripheral nerve regeneration: a systematic review. Bioengineering 5:44–56
16. Hashmi JT, Huang Y-Y, Osmani BZ et al (2010) Role of low-level laser therapy in neurorehabilitation. PM R 2:S292–S305
17. Coulthard P, Kushnerev E, Jm Y et al (2014) Interventions for iatrogenic inferior alveolar and lingual nerve injury. Cochrane Database Syst Rev 16:CD005293
18. Naftel JP, Richards LP, Pan M, Bernanke JM (1999) Course and composition of the nerves that supply the mandibular teeth of the rat. Anat Rec 256:433–447
19. Germanà G, Muglia U, Santoro M et al (1992) Morphometric analysis of sciatic nerve and its main branches in the rabbit. Biol Struct Morphog 4:11–15
20. Peng Q, Juzeniene A, Chen J et al (2008) Lasers in medicine. Rep Prog Phys 71:1–28
21. Rochkind S, Leider-Trejo L, Nissan M et al (2007) Efficacy of 780-nm laser phototherapy on peripheral nerve regeneration after neurotube reconstruction procedure (double-blind randomized study). Photomed Laser Surg 25:137–143
22. Andreo L, Soldera CB, Ribeiro BG et al (2017) Effects of photobiomodulation on experimental models of peripheral nerve injury. Lasers Med Sci 32:2155–2165
23. Gasperini G, De Siqueira ICR, Costa LR (2014) Lower-level laser therapy improves neurosensory disorders resulting from bilateral mandibular sagittal split osteotomy: a randomized crossover clinical trial. J Cranio-Maxillofacial Surg 42:e130–e133
24. Guarini D, Gracia B, Ramírez-Lobos V et al (2018) Laser biophotomodulation in patients with neurosensory disturbance of the inferior alveolar nerve after sagittal split ramus osteotomy: a 2-year follow-up study. Photomed Laser Surg 36:3–9
25. Alghamdi KM, Kumar A (2012) Low-level laser therapy : a useful technique for enhancing the proliferation of various cultured cells. Lasers Med Sci 27:237–249
26. Barez MM, Tajziehchi M, Heidari MH et al (2017) Stimulation effect of low level laser therapy on sciatic nerve regeneration in rat. J Lasers Med Sci 8:S32–S37
27. Wang CZ, Chen YJ, Wang YH et al (2014) Low-level laser irradiation improves functional recovery and nerve regeneration in sciatic nerve crush rat injury model. PLoS One 9:e103348
28. Takhtfooladi MA, Jahanbakhsh F, Takhtfooladi HA et al (2015) Effect of low-level laser therapy (685 nm, 3 J/cm2) on functional recovery of the sciatic nerve in rats following crushing lesion. Lasers Med Sci 30:1047–1052
29. Takhtfooladi MA, Sharifi D (2015) A comparative study of red and blue light-emitting diodes and low-level laser in regeneration of the transected sciatic nerve after an end to end neurorrhaphy in rabbits. Lasers Med Sci 30:2319–2324
30. Medalha CC, Di Gangi GC, Barbosa CB et al (2012) Low-level laser therapy improves repair following complete resection of the sciatic nerve in rats. Lasers Med Sci 27:629–635
31. Barbosa RI, Marcolino AM, De Jesus Guirro RR et al (2010) Comparative effects of wavelengths of low-power laser in regeneration of sciatic nerve in rats following crushing lesion. Lasers Med Sci 25:423–430
32. de Martins DO, dos Santos FM, de Oliveira ME et al (2013) Laser therapy and pain-related behavior after injury of the inferior alveolar nerve: possible involvement of neurotrophins. J Neurotrauma 30:480–486
33. de Martins DO, dos Santos FM, Ciena AP et al (2017) Neuropeptide expression and morphometric differences in crushed alveolar inferior nerve of rats: effects of photobiomodulation. Lasers Med Sci 32:833–840
34. Souza-Barros L, Dhaidan G, Maunula M et al (2018) Skin color and tissue thickness effects on transmittance, reflectance, and skin temperature when using 635 and 808 nm lasers in low intensity therapeutics. Lasers Surg Med 50:291–301
35. Nasouri B, Murphy TE, Berberoglu H (2014) Simulation of laser propagation through a three-layer human skin model in the spectral range from 1000 to 1900 nm. J Biomed Opt 19:075003
36. Miloro M, Criddle TR (2018) Does low-level laser therapy affect recovery of lingual and inferior alveolar nerve injuries? J Oral Maxillofac Surg 76:2669–2675
37. Miloro M, Halkias LE, Mallery S et al (2002) Low-level laser effect on neural regeneration in Gore-Tex tubes. Oral Surg Oral Med Oral Pathol Oral Radiol Endod 93:27–34
38. Angius D, Wang H, Spinner RJ et al (2012) A systematic review of animal models used to study nerve regeneration in tissue-engineered scaffolds. Biomaterials 33:8034–8039
39. Wang X, Reddy DD, Nalawade SS et al (2017) Impact of heat on metabolic and hemodynamic changes in transcranial infrared laser stimulation measured by broadband near-infrared spectroscopy. Neurophotonics 5(1):011004